Supporting Material for: Amplitude metrics for cellular circadian bioluminescence reporters

Peter C. St. John[1], Stephanie R. Taylor[2], John H. Abel[1], and Francis J. Doyle III[1,*]

[1]Department of Chemical Engineering, University of California Santa Barbara, Santa Barbara, California 93106-5080
[2]Department of Computer Science, Colby College, Waterville, Maine 04901
[*]Email: doyle@engineering.ucsb.edu

Model 1: Adapted from Novák & Tyson, 2008 (1). Model used for ARC demonstrations in Figs. 1-3, S1 ($P = 4$) and Fig. S2, Movies S1 & S2 ($P = 2$). It should be noted that the use of the stochastic simulation algorithm for reactions with non-elementary propensities may inaccurately represent the noise of the full system. In this case, we simply fit the noise characteristics of the approximated model (using the volume parameter) to yield physiologically realistic desynchronization rates. The volume of the stochastic simulations was chosen as $\Omega = 250$.

$$\frac{dX}{dt} = \frac{1}{1+Y} - X$$
$$\frac{dY}{dt} = k_t\, X - k_d\, Y - \frac{Y}{\alpha_0 + \alpha_1\, Y + \alpha_2 Y^2}$$

Parameter	Value
k_t	20
k_d	1
P	4 (or 2)

Parameter	Value
α_0	0.005
α_1	0.05
α_2	0.1

Model 2: Hirota *et al.* 2012 (2). A more detailed model of circadian rhythms used for simulations in Figs. 4-5.

$$\frac{d\,p}{dt} = \frac{-p \cdot vdp}{kdp + p} + \frac{vtp}{knp + (C1n + C2n)^3}$$
$$\frac{d\,c1}{dt} = \frac{-c1 \cdot vdc1}{c1 + kdc1} + \frac{vtc1}{knc1 + (C1n + C2n)^3}$$
$$\frac{d\,c2}{dt} = \frac{-c2 \cdot vdc2}{c2 + kdc1} + \frac{vtc2}{knc1 + (C1n + C2n)^3}$$
$$\frac{d\,P}{dt} = -C1 \cdot P \cdot vaC1P + C1n \cdot vdC1P - C2 \cdot P \cdot vaC1P + C2n \cdot vdC1P - \frac{P \cdot vdP}{P + kdP} + ktxnp \cdot p$$
$$\frac{d\,C1}{dt} = -C1 \cdot P \cdot vaC1P - \frac{C1 \cdot vdC1}{C1 + kdC1} + C1n \cdot vdC1P + c1$$
$$\frac{d\,C2}{dt} = -C2 \cdot P \cdot vaC1P - \frac{C2 \cdot vdC2}{C2 + kdC1} + C2n \cdot vdC1P + c2$$
$$\frac{d\,C1n}{dt} = C1 \cdot P \cdot vaC1P - C1n \cdot vdC1P - \frac{C1n \cdot vdCn}{C1n + C2n + kdCn}$$
$$\frac{d\,C2n}{dt} = C2 \cdot P \cdot vaC1P - \frac{C2n \cdot MC2n \cdot vdCn}{C1n + C2n + kdCn} - C2n \cdot vdC1P$$

Parameter	Value
vtp	0.195
$vtc1$	0.131
$vtc2$	0.114
knp	0.425
$knc1$	0.259
vdp	0.326
$vdc1$	0.676

Parameter	Value
$vdc2$	0.608
kdp	0.0115
$kdc1$	1.15
vdP	2.97
$vdC1$	0.0338
$vdC2$	1.52
$vdCn$	1.69

Parameter	Value
$MC2n$	2.02
kdP	0.101
$kdC1$	3.32
$kdCn$	0.0526
$vaC1P$	0.0406
$vdC1P$	0.00175
$ktxnp$	3.0

Model 3: The Oregonator model (3), with parameters as presented in (4). Used in Fig. S3 as an example of a limit cycle oscillator using only mass-action kinetics.

The individual chemical reactions (used for stochastic simulation) are:

$$
\begin{aligned}
X_1 + Y_2 &\xrightarrow{c_1} Y_1 \\
Y_1 + Y_2 &\xrightarrow{c_2} Z_1 \\
X_2 + Y_1 &\xrightarrow{c_3} 2Y_1 + Y_3 \\
2Y_1 &\xrightarrow{c_4} Z_2 \\
X_3 + Y_3 &\xrightarrow{c_5} Y_2
\end{aligned}
$$

These reactions can be converted to a standard ODE model, in which only the intermediate variables Y are considered, as:

$$
\begin{aligned}
\frac{dY1}{dt} &= c1x1 \cdot Y2 - c2 \cdot Y1 \cdot Y2 + c3x2 \cdot Y1 - c4 \cdot Y1^2 \\
\frac{dY2}{dt} &= -c1x1 \cdot Y2 - c2 \cdot Y1 \cdot Y2 + c5x3 \cdot Y3 \\
\frac{dY3}{dt} &= c3x2 \cdot Y1 - c5x3 \cdot Y3
\end{aligned}
$$

Parameter	Value
$c1x1$	2
$c2$	0.1
$c3x2$	104
$c4$	0.016
$c5x3$	26

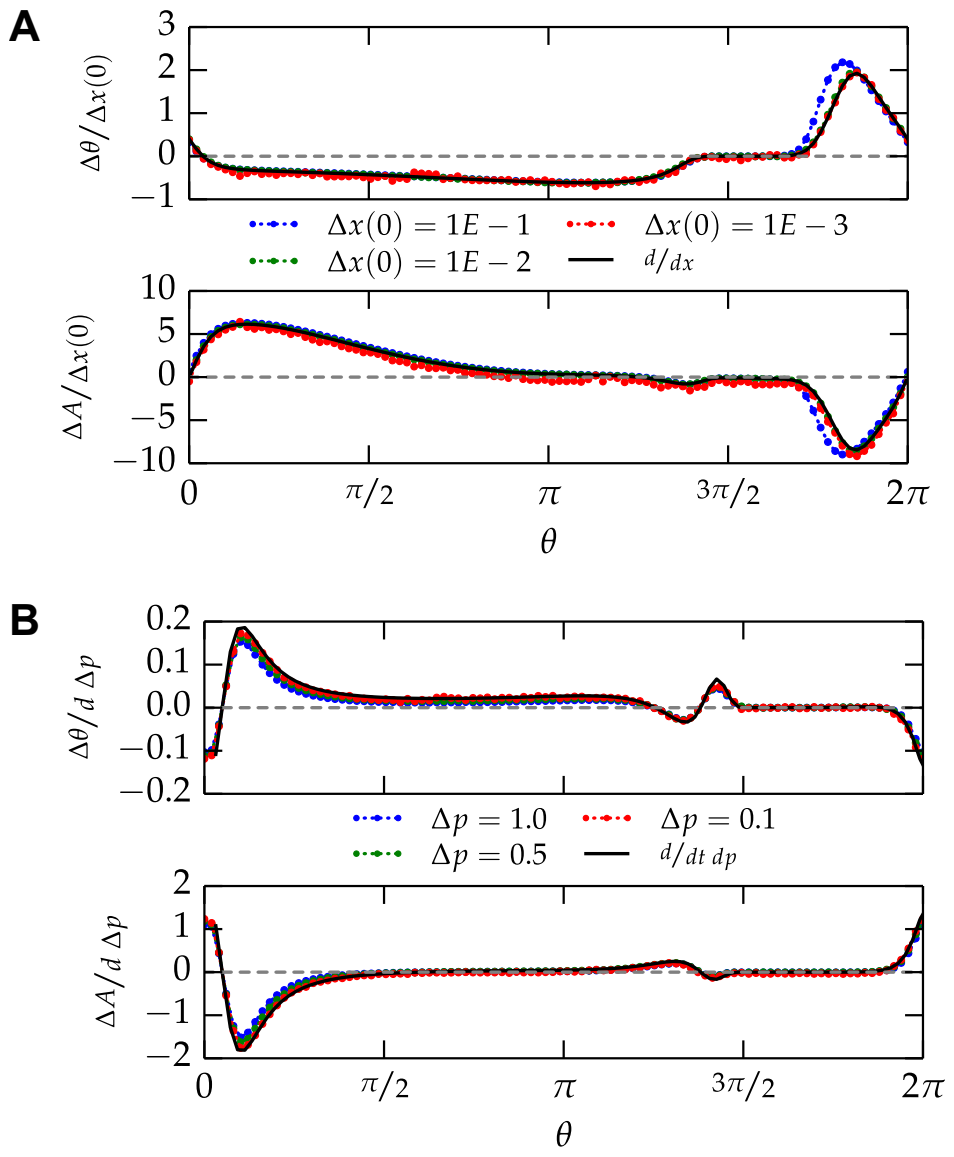

Figure S1: Convergence of finite-difference and differential methods. (**A**) Perturbations of decreasing strength to the state of the oscillator result in phase and amplitude response curves that match the differential limit. (**B**) Temporary perturbations of decreasing strength to a kinetic parameter. The duration of each perturbation is fixed to 0.2 radians. Finite difference approximations closely match the differential method, which is offset in phase by 0.1 radians to account for the nonzero pulse duration.

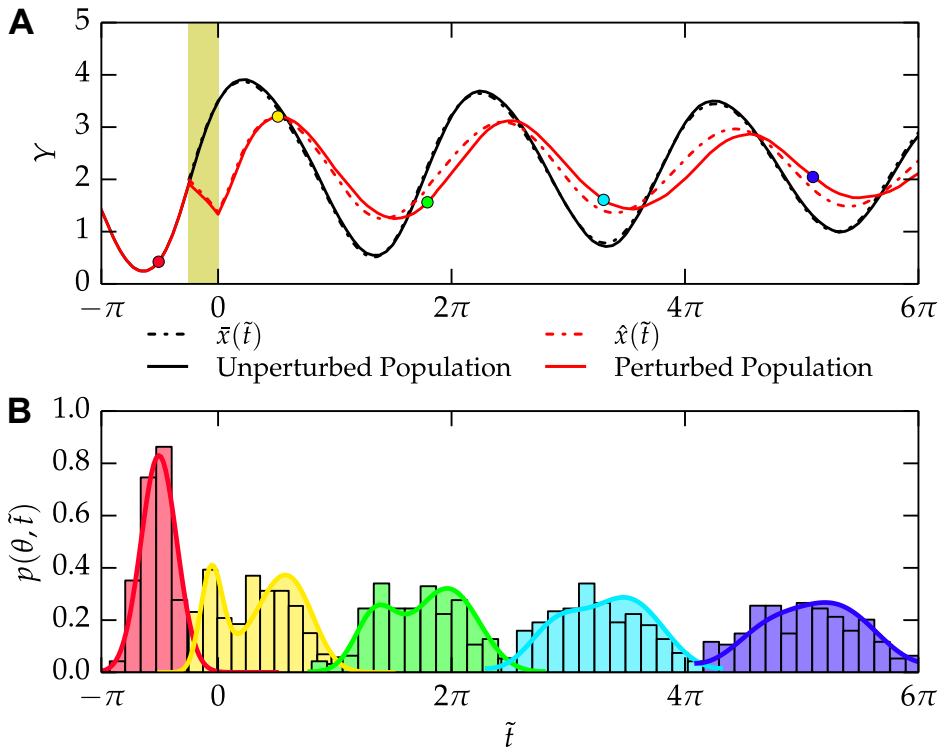

Figure S2: Approximation of an explicit stochastic population by continuous methods. (**A**) A population of 225 stochastic oscillators was simulated using the Gillespie stochastic simulation algorithm (SSA), see Movie S1 and S2. The mean protein expression, Y, is plotted as a function of time. A 50% reduction in the protein translation rate to each of the oscillators is applied from $\hat{t} = -\pi/4 \rightarrow 0$, resulting in both single-cell and population-level amplitude change (red solid line). This population is approximated by the continuous methods described in this manuscript, in which the decay parameter $d = 0.025$ is estimated to match the stochastic-induced desynchrony of the control population (black solid line). The initial standard deviation $\sigma_0 = 0.48$ is similarly matched to the stochastic population. The resulting predicted unperturbed and perturbed trajectories, $\bar{x}(\hat{t})$ and $\hat{x}(\hat{t})$ respectively, closely match the stochastically modeled values. (**B**) Phase histograms for the stochastic population are shown at several phases, both before and after the desynchronizing perturbation. Phase probability-density functions for the continuous approximation are also shown, with close agreement between stochastic and continuous simulations. This close approximation validates the use of ODE models and phase-diffusion populations in deriving amplitude and phase-response behavior for networks of uncoupled cells.

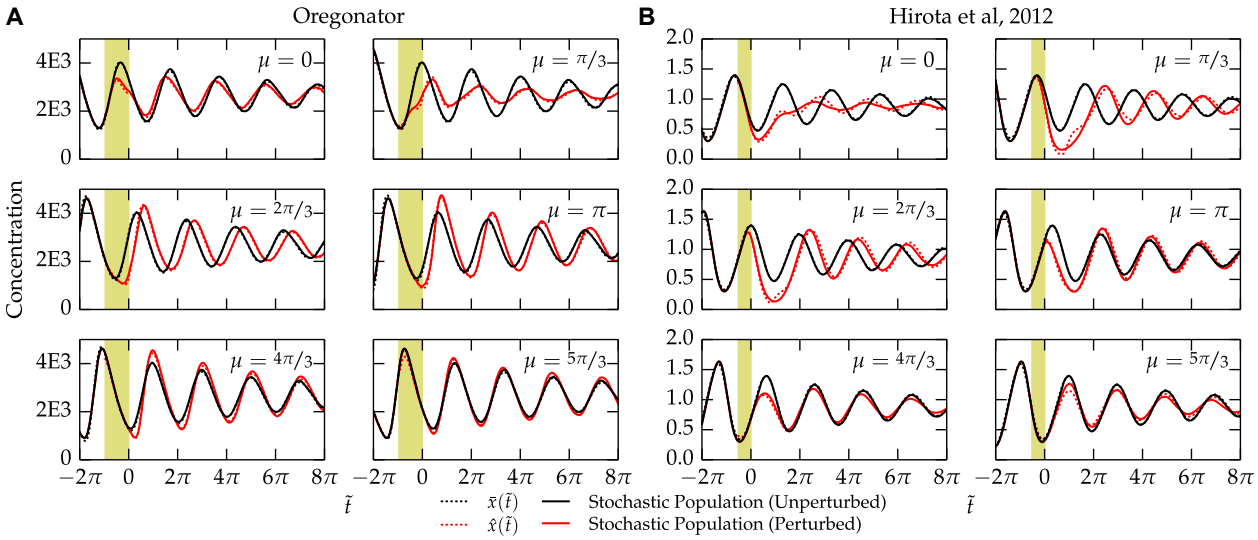

Figure S3: Validation of continuous methods with alternate models. (**A**) The Oregonator model (Model 3) was tested as an example of a mass-action limit cycle oscillator. A population of 2000 oscillators was perturbed at size different mean phases, μ, by increasing the *c2* parameter by 50% for $d = \pi$ (highlighted region). Only the average *Y2* variable is plotted. (**B**) The model described in (2) (Model 2) was similarly tested at a variety of mean phases by reducing the *vdp* parameter by 28.5% and plotting the resulting *c2* state variable (as in Fig. 5). Parameters for the continuous approximations were found by estimating the phase, initial standard deviation, period, and phase diffusivity of the control population. Good agreement is seen between the continuous and stochastic simulations, indicating the proposed method is suitable for predicting the population-level responses for a variety of model types. The slightly reduced accuracy seen in the larger Model 2 demonstrates a limitation of the method, which should be considered before applying the method to extreme cases. As Eq. 44 tabulates the response of the system from the limit cycle, systems which are perturbed from states far from the deterministic limit cycle will not be captured appropriately. Therefore, the difference in accuracy between Model 2 and Model 3 likely comes from increased deviation about the deterministic limit cycle in a greater number of spatial dimensions.

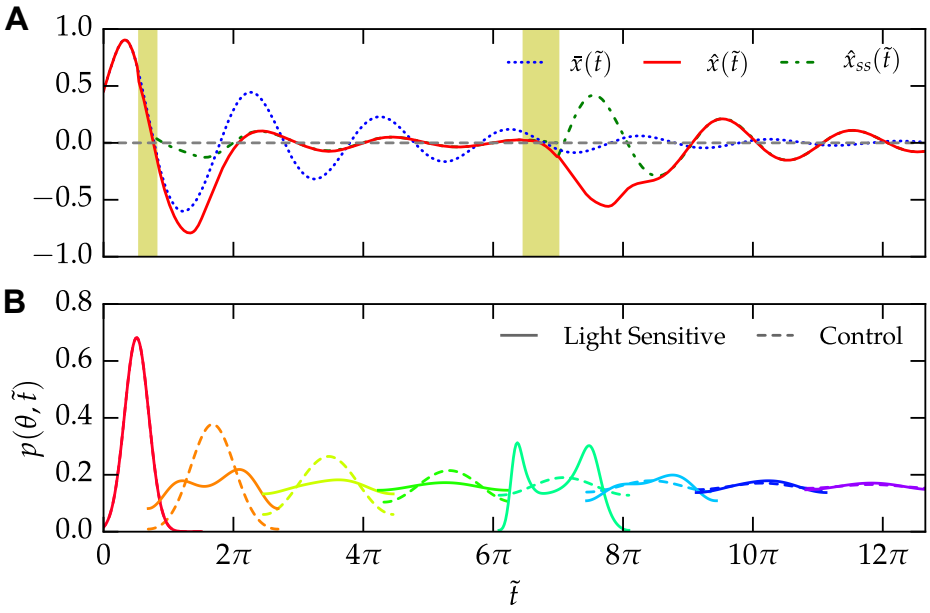

Figure S4: Evidence of single-cell and population-level amplitude change. (**A**) The simulated control trajectory as shown in Fig. 5 is plotted again as $\bar{x}(\tilde{t})$. The simulated light-sensitive trajector is also replotted as $\hat{x}(\tilde{t})$, which incorperates both single-cell and population-level effects. The difference between this trajectory and the steady-state perturbed trajectory following both pulses, $\hat{x}_{ss}(\tilde{t})$, demonstrates the effect of single-cell level amplitude change in this particular case. Single-cell amplitudes are greatly increased following the first pulse, and altered significantly following the second. (**B**) Comparison of the population densities for the control (dashed) and perturbed (solid) simulations. The perturbed population is greatly desynchronized following the first light pulse, as indicated by its flatness relative to the control population. Following the second pulse, the perturbed population is more concentrated than the control, indicating higher amplitudes. These comparisons demonstrate the changes in population synchrony which occur due to the light pulse.

Movie S1: Stochastic simulation of a two-state limit cycle oscillator. A population of 225 stochastic oscillators was simulated using the Gillespie stochastic simulation algorithm (SSA). The deterministic limit cycle, $x^{\gamma}(\hat{t})$, is shown in black (left), and the current location of individual stochastic oscillators are shown by green dots. The population average, plotted in both the state (left) and time (right) domains, is shown in red. Stochastic noise drives the population to gradually desynchronize, resulting in damped oscillations of the average protein level.

Movie S2: Perturbation to a population of stochastic oscillators. The population of oscillators is perturbed by a 50% reduction in the protein translation rate to each of the oscillators from $\hat{t} = -\pi/4 \rightarrow 0$ (yellow frames), resulting in both single-cell and population-level amplitude change. The oscillators quickly recover to the limit cycle (single-cell level amplitude change), but the population is left desynchronized (population-level amplitude change).

Supporting References

1. Novák, B., and J. J. Tyson, 2008. Design principles of biochemical oscillators. *Nat. Rev. Mol. Cell Biol.* 9:981–991.

2. Hirota, T., J. W. Lee, P. C. St. John, M. Sawa, K. Iwaisako, T. Noguchi, P. Y. Pongsawakul, T. Sonntag, D. K. Welsh, D. A. Brenner, F. J. Doyle III, P. G. Schultz, and S. A. Kay, 2012. Identification of Small Molecule Activators of Cryptochrome. *Science* 337:1094–1097.

3. Field, R. J., and R. M. Noyes, 1974. Oscillations in chemical systems. IV. Limit cycle behavior in a model of a real chemical reaction. *J. Chem. Phys.* 60:1877.

4. Gillespie, D. T., 1977. Exact Stochastic Simulation of Coupled Chemical Reactions. *J. Phys. Chem.* 84:2340–2361.